Eur. Phys. J. Special Topics **222**, 1563–1573 (2013)
© EDP Sciences, Springer-Verlag 2013
DOI: 10.1140/epjst/e2013-01945-5

THE EUROPEAN PHYSICAL JOURNAL SPECIAL TOPICS

Regular Article

Dynamic isolation systems using tunable nonlinear stiffness beams

M.I. Friswell[1,a] and E.I. Saavedra Flores[2]

[1] College of Engineering, Swansea University, Singleton Park, Swansea SA2 8PP, UK
[2] Departamento de Ingeniería en Obras Civiles, Universidad de Santiago de Chile, Av. Ecuador 3659, Santiago, Chile

Received 4 June 2013 / Received in final form 2 August 2013
Published online 30 September 2013

Abstract. Vibration isolation devices are required to reduce the forcing into the supporting structure or to protect sensitive equipment from base excitation. A suspension system with a low natural frequency is required to improve isolation, but with linear supports the minimum stiffness is bounded by the static stiffness required to support the equipment. However, nonlinear high-static-low-dynamic-stiffness (HSLDS) mounts may be designed, for example by combining elastic springs in particular geometries, to give the required nonlinear force-displacement characteristics. Current approaches to realise the required nonlinear characteristics are often inconvenient. Furthermore, the weight of the supported equipment, the environment, or the structural stiffness may change. This paper investigates the design of HSLDS isolation mounts using beams of tunable geometric nonlinear stiffness. In order to obtain the nonlinear response required, we first study the case of generic beams subject to static loads that are able to tune their nonlinear force-displacement characteristics to ensure that the isolators have very low dynamic stiffness. Tuning is achieved by actuators at the ends of the beams that prescribe the axial displacement and rotation. Secondly, we study a composite beam with an initial thermal pre-stress, resulting in internal stresses that give the required nonlinear response.

1 Introduction

The dynamics of rotating machinery, and in particular the response to out-of-balance forces and moments [1,2], can produce significant forcing into the supporting structure. To reduce the force transmission the machine may be supported on isolation mounts [3,4], and their performance is directly related to the low linear stiffness of the mounts. Isolation mounts are also used to isolate sensitive equipment from base excitation from the supporting structure. However, a low stiffness for good isolation conflicts with the requirement of the mounts to support the weight of the machine or equipment. In this paper mounts with nonlinear force-displacement characteristics are exploited to solve this dilemma.

[a] e-mail: m.i.friswell@swansea.ac.uk

The use of suspension systems with a low natural frequency is of great interest in a range of applications. For example, zero-length springs may be used to measure gravity [5] or devices with low natural frequencies may be used to simulate zero-gravity experiments [6,7]. Low stiffness supports are also required for free-free vibration testing [8,9]. A major field of applications for systems with low natural frequencies is vibration isolation, for example in vehicle driver isolation [10]. In this case, a certain static stiffness must be provided to prevent a large static displacement to occur. For this reason systems referred to as high-static-low-dynamic-stiffness (HSLDS) isolation mounts are particularly interesting. Alabuzhev et al. [11] gave different strategies to realise an HSLDS characteristic for vibration protection systems. The principle is to combine elastic elements (e.g. springs) in a particular manner to give the required parallel combination of elements with negative and positive stiffness. In doing so, the total stiffness can be made as small as desired, and theoretically can be zero. Carrella et al. [12–14] analysed the static and dynamic characteristics of systems with HSLDS mechanisms for vibration isolation purposes and demonstrated that these can reduce the natural frequency without paying the usual penalty of a high static displacement. In theory it is possible to design suspension systems with zero dynamic stiffness (also referred to as quasi-zero-stiffness, QZS, mechanisms) but these have the significant drawback that any changes in the design, for example due to manufacturing tolerances, can result in negative stiffness, i.e. an unstable system [15]. Carrella et al. [16] considered the vibration isolation of a rotating machine and the effect of large displacements.

The physical realisation of the nonlinear force-displacement characteristic is a difficult task. Platus [17] used beam buckling to provide the required negative stiffness, with the positive stiffness provided by a conventional support spring. Robertson et al. [18,19] used inclined permanent magnets. Jutte and Kota [20,21] designed compliant mechanisms to synthesise the required force-displacement characteristic. Keye et al. [22] applied an axial load to a beam to reduce the stiffness of a vibration absorber. The method proposed in this paper is to apply internal stresses within a beam to obtain the required characteristics. These stresses may arise from external loads or prescribed displacements, or may be obtained from residual stresses after curing in a composite beam or plate. Most applications have considered bistable composite structures [23], which give nonlinear stiffness characteristics, although the linear stiffness component would have to be increased for vibration isolation applications and to obtain the desired stiffness characteristics [24,25].

A further problem with nonlinear vibration absorbers is the requirement to tune the force-displacement characteristics to ensure that the isolator has very low dynamic stiffness despite variation in the structural parameters, the environment or the static loads. Tuning the stiffness has been important for vibration absorbers where the natural frequency has to match the excitation frequency [26], although the static load is not usually important for these systems. Keye et al. [22] used axial loads to tune a vibration absorber.

Approaches will be described in this paper to tune the force-displacement characteristic by varying the boundary conditions and residual stress of a beam. The objective is to produce an isolator that may be implemented by a much simpler structure than existing isolators. Ultimately one could imagine a leaf spring designed and tuned to give the required force displacement characteristics.

2 Linear vibration isolation

To illustrate the properties of a linear vibration isolator we consider a mount modelled as a spring and dashpot, that supports a rigid mass. This single degree of freedom

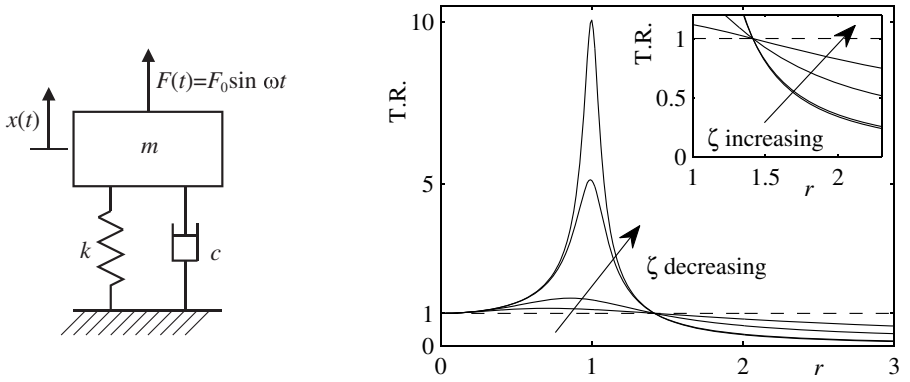

(a) Schematic of system

(b) Transmission ratio (T.R.) for $\zeta = 0.05, 0.1, 0.5, 1.0$

Fig. 1. Vibration isolation properties of a linear mount.

system illustrates the important properties that the mount stiffness plays in the isolation performance. Figure 1(a) shows a schematic of the mount. Inman [3] analysed the equations of motion of this system subjected to a force $F_0 \sin \omega t$ on the mass. The transmitted force is

$$F_T(t) = kx(t) + c\dot{x}(t). \tag{1}$$

The amplitude of $F_T(t)$, denoted F_{T0}, may be calculated and expressed as the *transmission ratio*

$$\text{T.R.} = \frac{F_{T0}}{F_0} = \sqrt{\frac{1 + (2\zeta r)^2}{(1 - r^2)^2 + (2\zeta r)^2}} \tag{2}$$

where ζ is the damping ratio ($\zeta = c/(2\sqrt{mk})$), $r = \omega/\omega_n$ and $\omega_n = \sqrt{k/m}$ is the natural frequency. Fig. 1(b) shows the transmission ratio for various excitation frequencies and damping ratios and highlights that this ratio is less than 1 for $r > \sqrt{2}$. Hence a high value of r gives a low force transmission and for a given mass and excitation frequency this high value of r is obtained by a low mount stiffness. A similar analysis may be performed for displacement transmissibility for a moving base [3].

3 Nonlinear isolation mounts

As mentioned in the introduction, it is possible to design a nonlinear suspension system which has a low dynamic stiffness, and thus a low natural frequency for oscillations about its static equilibrium position, without having to compromise on the static displacement (HSLDS springs) [4,11]. The solid line in Fig. 2 shows the desired nonlinear force-deflection curve together with that of a linear spring (dashed). The static equilibrium position (after the static load has been applied, which is usually the weight of the machine, W) is x_e for both mounts. However, for oscillation about this point the dynamic stiffness (local slope of the curve) is smaller than that of the linear spring, which implies that the natural frequency is also lower. For small oscillations a linear behaviour can be assumed. Carrella et al. [16] considered the nonlinear dynamics of a rotating machine when the displacements were large.

Various approaches to realise the required nonlinear force displacement characteristic were discussed in the introduction. For illustration we consider a system using linear elastic springs shown in Fig. 3 [15]. The oblique springs with equal coefficients

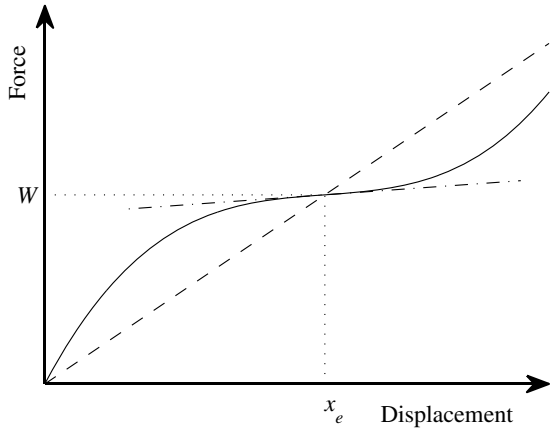

Fig. 2. The force-displacement characteristic of a linear (dashed) and a nonlinear (solid) spring. At equilibrium the static stiffness of the linear and nonlinear springs are equal, but the dynamic stiffness of the nonlinear spring (the slope given by the dot-dash line) is much smaller. x_e is the equilibrium displacement for the static load W.

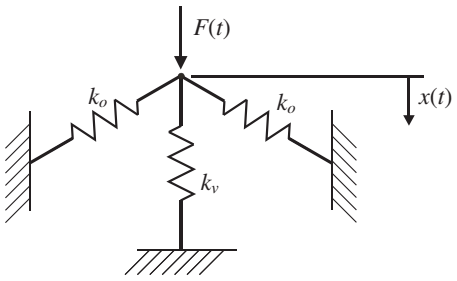

Fig. 3. Schematic representation of a mechanism with HSLDS characteristics: the oblique springs provide the necessary negative stiffness, whilst the vertical spring gives the positive stiffness.

k_o act as *negative* stiffness elements, and are connected in parallel to a vertical spring of (positive) stiffness, k_v. Considering the motion about the equilibrium position, the effective nonlinear load-deflection characteristic can be approximated to a cubic function of displacement

$$F(x) = k_1 (x - x_e) + k_3 (x - x_e)^3 \tag{3}$$

where k_1 and k_3 depend on the initial angle of the oblique springs and on the coefficients of the three springs. Here we assume that $k_3 > 0$, and hence the spring has a hardening characteristic. Different systems with a softening stiffness, $k_3 < 0$, can be also designed, although these systems are not so useful for vibration isolation. When $k_1 = 0$ the slope at x_e (as in Fig. 2) is zero and the system becomes a QZS mechanism. The system can be designed so that the static equilibrium position occurs when the oblique springs are horizontal.

4 Models and applications of bistable plates

Multi-stable structures provide alternative structural configurations to realise large changes in the geometry without using discretely hinged rigid bodies. Bistable or multi-stable structures are obtained by introducing a residual stress field into the structure through pre-stress or through thermal stresses. Thermally induced bistable composites may be obtained using unsymmetric laminates made of orthotropic material, which exhibit out-of-plane displacements at room temperature even if cured flat. These displacements are caused by residual stress fields induced during the cool-down process between the highest curing temperature ($\approx 160\,^\circ$C) and room temperature ($\approx 20\,^\circ$C). The thermal stresses are mainly caused by the mismatch of the coefficients

of thermal expansion of constituent layers. During the cool-down in the manufacturing process a residual stress field is locked into the laminate and the unsymmetric stacking sequence produces moments that result in out-of-plane displacements. The main characteristic of unsymmetric laminates is that the internal stresses have more than one position of equilibrium making them bistable or multi-stable. This creates structures that can be at the same time flexible and stiff and opens up the possibility of combining several bistable components to obtain structures with multiple configurations. Diaconu et al. [27] investigated different concepts to introduce multi-stable structures into aircraft systems and Mattioni et al. [23] simulated bistable structures using finite element analysis.

The main feature of a bistable structure is the snap-through mechanism which marks the passage from one stable position to the other. Suppose that a square bistable plate has pinned supports at its four corners and a load is applied at the centre of the plate. Then the force-displacement characteristic is approximately a cubic [24], although the bistable nature of the plate means that the stiffness is negative when the plate is approximately flat. To obtain the required characteristics for a vibration isolator a positive linear stiffness is required, and this may be realised either by an external spring or by optimising the layup of the plate. Bistable plates are often inconvenient for use as mounts because significant deformation is required at the edges of the plate. If the edges are fixed then this will affect the bistable behaviour. However these structures motivate the investigation of composite beams with internal and external forces and moments.

5 Isolation mounts realised using beams

A simple example will be used to motivate the use of beams to realise the vibration mounts. Two principles will be used to tailor the beam properties to obtain the nonlinear force-displacement response required, as shown in Fig. 2. The cubic hardening nonlinearity uses the geometry nonlinearity for beams with pinned or fixed ends undergoing large displacements. Internal stresses are used to reduce the linear stiffness and to tune the point of inflection on the force-displacement curve to the required static load. These internal stresses are implemented in this simple example by a prescribed axial displacement at one end of the beam and prescribed rotations at both ends of the beam. Figure 4 shows this schematically. Equal imposed rotations at both ends of the beam will produce a symmetric deformation, which is preferable to an asymmetric deformation that would give a rotation of the beam at the point of application of the external load. Although the imposed axial displacement is shown at one end of the beam, in practice this displacement would be imposed at both ends of the beam so that the point of application of the external load does not move laterally.

At the boundaries one has the choice of imposing constraints on the translation and rotation, or applying forces and moments. These two approaches are equivalent for a single load case, providing the beam does not buckle. If the beam buckles then only one of the multiple solutions would be obtained. However, for vibration about the equilibrium position, the two approaches will give slightly different linear stiffness values. Furthermore, imposing boundary conditions is more suitable for structures that buckle, since the conventional force approach is unable to obtain all of the solution branches and more advances approaches, such as the arc-length method, are required. The realisation of the beam isolator will require actuators and a control system, and the most appropriate model for the end conditions will depend on the implementation adopted. For example, if the actuators were very stiff, then imposing boundary displacements and rotations is the most appropriate model.

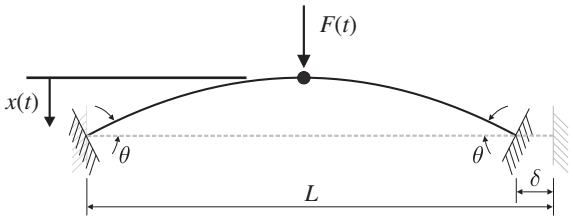

Fig. 4. Schematic of the beam subjected to prescribed axial displacement, δ, and rotation, θ, at both ends of the beam, followed by a prescribed transverse displacement at the beam centre. The beam is clamped once the prescribed axial displacement and rotation have been applied.

The beam is initially flat with no internal stresses (shown by the grey dashed line in Fig. 4). The axial displacement and rotations at the ends of the beam are then applied, introducing residual stresses and causing the beam to deform (shown by the solid line). The force displacement characteristics are then obtained by prescribing a centre displacement, $x(t)$, and determining the corresponding transverse reaction load at the centre of the beam, $F(t)$.

The example beam has length $L = 1.0\,\text{m}$, and a circular cross-section with diameter $d = 0.01\,\text{m}$. Note that in practice the beam is likely to have a rectangular section although for this illustration the cross-section shape is not important. The Young's modulus is $E = 200\,\text{GPa}$ and the Poisson's ratio is $\nu = 0.3$. The reaction load at the middle of the beam, at the node where the vertical displacement is applied, is normalised by the factor $\dfrac{48EI}{L^3}x_0$, where $x_0 = 1\,\text{m}$ is a unit displacement. The displacements are prescribed at the centre of the beam and are normalised by the length of the beam, L. For all cases, the beams were modelled in ANSYS. Each model consisted of 31 nodes and 30 `BEAM188` type elements, with cubic interpolation, based on Timoshenko beam theory. This type of element is particularly well-suited to large deflection, large rotation and/or large strain nonlinear applications. Local instabilities developed during the non-linear deformation process, and hence the automatic stabilisation method provided by ANSYS was used in order to capture the buckling and post-buckling response. Large displacement theory was applied at all times.

The loading programme starts with a beam that is initially straight. Rotations at both ends of the beam are applied gradually in 5 load steps. The axial compressive displacement is then applied, also in 5 load steps. Finally, the prescribed vertical displacement is applied in 40 load steps. Figure 5 shows the force displacement response as the prescribed axial displacement is varied for a fixed prescribed rotation of $\theta = 6°$. For low prescribed displacements the response is almost linear. However increasing the prescribed displacements, increases the internal stresses, and reduces the localised stiffness. For large prescribed displacements the beam buckles, as shown by the regions of negative stiffness. Figure 6 shows the force displacement response as the prescribed rotation is varied for a fixed prescribed axial displacement of $\delta = 0.001L$. The mount characteristics again look approximately cubic, although the form is sightly different to Fig. 5. The beam buckles for low values of prescribed rotation, and clearly there is a prescribed rotation that will give a zero linear stiffness.

In practice one would choose the prescribed axial displacement and rotation at the end of the beam so that the point of inflection occurs at the static load and to give the required linear stiffness. It is clear from Figs. 5 and 6 that θ and δ both affect the load carried by the isolator and the stiffness, and that the optimum solution for θ and δ will be unique. As an example, suppose that the linear stiffness is required to be zero. For a given prescribed rotation, the prescribed axial displacement may be chosen to give zero linear stiffness. Figure 7 shows the results obtained for three

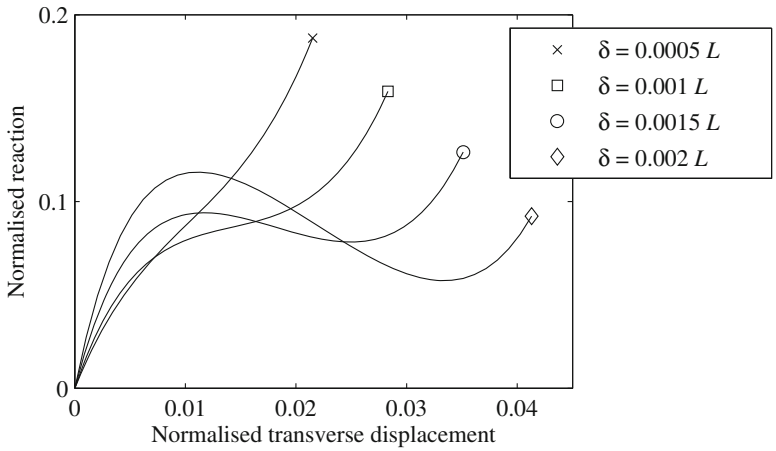

Fig. 5. Influence of prescribed axial displacement at the ends of the straight beam. The prescribed rotation is $\theta = 6^\circ$.

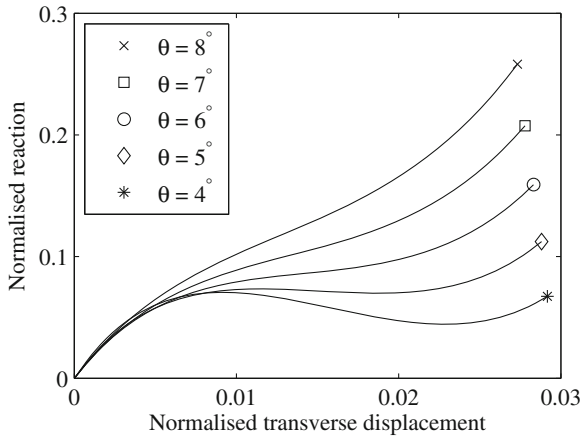

Fig. 6. Influence of prescribed rotation at the ends of the straight beam. The prescribed axial displacement is $\delta = 0.001L$.

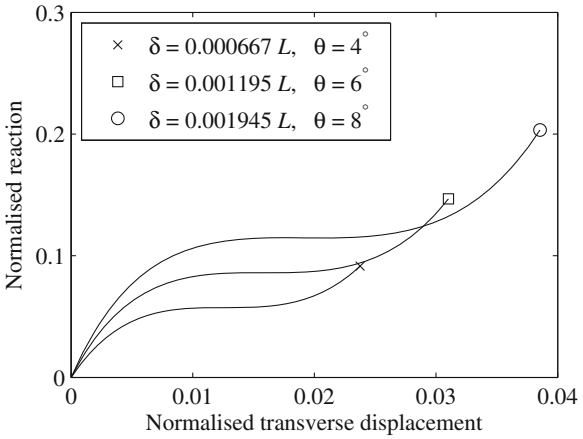

Fig. 7. Various choices of prescribed axial displacement and rotation that give a zero linear stiffness.

Table 1. The variation of the optimum θ and δ with static load.

Static load (Normalised)	θ	δ
0.057	4°	$0.000667L$
0.086	6°	$0.001195L$
0.115	8°	$0.001945L$

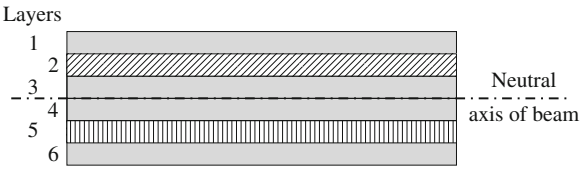

Fig. 8. A schematic of the composite beam with 6 layers. The coefficient of thermal expansion for layers 2 and 5 are different to that of the other layers.

choices of prescribed rotation and Table 1 shows how θ and δ change with the applied static load. This clearly demonstrates that the system may be tuned to cope with a wide variety of static loads by the appropriate choice of prescribed axial displacement and rotation at the end of the beam.

6 Beams with internal stresses due to thermal effects

Applying external forces and moments to the end of a beam results in a complex system. Often isolators are required that are relatively simply devices, and one option is to introduce internal stresses into the beam. Hence, in this section, we investigate the nonlinear response of a composite beam with an unsymmetric distribution of coefficients of thermal expansion through its layers. As commented earlier, due to the mismatch of the thermal coefficients in the constituent layers, a residual stress field is created when a thermal gradient is applied to the beam, resulting in a new initial pre-stressed condition.

The design of a composite beam to produce the required internal forces and moments is not unique. At least two layers are required, but often the ply thickness is relatively small and so more layers are required to carry the applied loads. Residual stresses in the outer layers will generate a greater moment, and so these layers are preferred for the material with a different coefficient of thermal expansion. However, the different coefficients of thermal expansion often occur because of the different ply angles and the differing thermal properties of the fibre and the matrix. A detailed design of the beam would have to address both the mechanical properties of the beam as well as the induced residual stresses. To illustrate that a composite beam is able to produce the required force displacement characteristics, a simple example is considered here. This example consists of a simply supported beam of 1 m length, with a rectangular cross-section of 30 mm height. The composite beam comprises six internal layers of 5 mm thickness, numbered from 1 to 6, from top to bottom. For illustrative purposes, all of the layers have the same Young's modulus of $E = 200$ GPa and Poisson's ratio of $\nu = 0.3$. For layers 1, 3, 4 and 6, a coefficient of thermal expansion of $10^{-7}/^\circ$C is chosen. For layers 2 and 5 we adopt values of $10^{-4}/^\circ$C and $10^{-8}/^\circ$C, respectively. The composite beam is shown schematically in Fig. 8.

The finite element model consists of 4207 nodes and 3600 `PLANE182` type elements which are defined by four nodes with two degrees of freedom at each node. For all

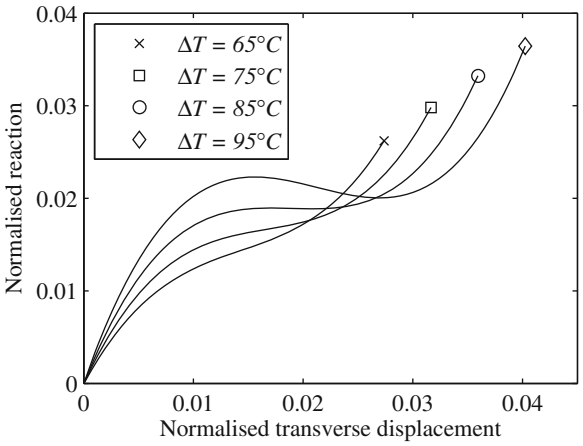

Fig. 9. The force-displacement response as a function of the initial thermal gradient, ΔT.

of the analyses, a plane stress formulation is adopted. The loading programme begins when the beam is initially straight. Then, the thermal gradient, ΔT, is applied in 5 load steps as an uniform body force load assigned to all the nodes. Once the new thermally induced equilibrium position is reached, the prescribed vertical displacement is applied in 40 load steps at the centre of the beam. Figure 9 shows the force-displacement response as the initial thermal gradient is varied from 65 to 95°C. Similarly to the previous examples, the reaction load and the prescribed displacements at the centre of the beam are normalised.

Within a range of small normalised displacements (smaller than 0.01), the response becomes stiffer as the initial gradient ΔT increases. This trend is explained by the fact that, by increasing ΔT, the curvature of the beam increases and therefore its initial stiffness also increases. For an increase in the temperature equal to approximately 85 °C, the graph shows a zero linear stiffness for normalised displacements close to 0.02. For larger thermal gradients the beam buckles. These results show that the HSLDS characteristic may be designed by tailoring the residual stresses for a given static load, although some active control would be required if the load or environment changed significantly.

7 Conclusions

The results in this paper have demonstrated that the linear stiffness and the point of inflection in the force-displacement characteristic for the beam isolator may be tuned by prescribing the displacement and rotation at the ends of the beam. This produces internal stresses within the beam that give the required response. Alternatively these internal stresses may be incorporated within a composite beam to give a distributed force and moment on the beam. The method of manufacture would most likely require pre-stress of the composite beam, or would require a layup significantly different to that used for bistable plates. If the static load for a particular vibration isolation application is known and constant then using residual stresses to give the required force-displacement characteristic has the great advantage that the supports could then be very simple.

If the static load or the structural parameters change, for example due to operational requirements or environmental conditions, then the vibration isolator would

have to tune its stiffness so that the point of inflection occurred at the equilibrium position of the system. This tuning could be achieved by actuators at the ends of the beam to prescribe the axial displacement and the rotation. Piezoelectric stack actuators would be a good choice since they are stiff and the required displacements are small. Alternatively piezoelectric or shape memory alloys actuators could be distributed within the composite beam.

The authors also acknowledge the support received from the European Research Council (ERC). The research leading to these results has received funding from the ERC under the European Union's Seventh Framework Programme (FP/2007-2013) / ERC Grant Agreement No. [247045]. E.I. Saavedra Flores also acknowledges the support of the Department of Civil Engineering, University of Santiago, Chile.

References

1. M.I. Friswell, J.E.T. Penny, S.D. Garvey, A.W. Lees, *Dynamics of Rotating Machines* (Cambridge University Press, 2010)
2. G. Genta, *Vibration of Structures and Machines: Practical Aspects* (Springer-Verlag, 1995)
3. D.J. Inman, *Engineering Vibrations*, 3rd edn. (Pearson, 2008)
4. E.I. Rivin, *Passive Vibration Isolation* (Wiley-Blackwell, 2003)
5. L. Lacoste, Physics **5**, 178 (1934)
6. M.S. Whorton, *g-limit: A microgravity vibration isolation system for the international space station*, in Spacebound 2000, Vancouver, BC, 14–17 May (2000)
7. K.K. Denoyer, C. Johnson, *Recent achievements in vibration isolation systems for space launch and on-orbit applications*, in 52nd International Astronautical Congress, Toulouse, France, 1–5 October (2001)
8. D.J. Ewins, *Modal Testing: Theory, Practice and Application*, 2nd edn. (Research Studies Press, 2000)
9. T.G. Carne, D.T. Griffith, M.E. Casias, *Support conditions for free boundary-condition modal testing*, in *Proceedings of IMAC XXV*, Orlando, Florida, 19–22 February (2007), Paper No. 295
10. C.-M. Lee, V.N. Goverdovskiy, A.I. Temnikov, J. Sound Vibr. **302**, 865 (2007)
11. P. Alabuzhev, A. Gritchin, L. Kim, G. Migirenko, V. Chon, P. Stepanov, *Vibration Protecting and Measuring Systems with Quasi-Zero Stiffness* (Hemisphere Publishing, NY, 1989)
12. A. Carrella, M.J. Brennan, T.P. Waters, V. Lopes, Int. J. Mech. Sci. **55**, 22 (2012)
13. A. Carrella, M.J. Brennan, I. Kovacic, T.P. Waters, J. Sound Vibr. **322**, 707 (2009)
14. A. Carrella, M.J. Brennan, T.P. Waters, J. Mech. Sci. Technol. **21**, 946 (2007)
15. A. Carrella, M.J. Brennan, T.P. Waters., J. Sound Vibr. **301**, 678 (2007)
16. A. Carrella, M.I. Friswell, A. Zotov, D.J. Ewins, A. Tichonov, Mech. Syst. Signal Proc. **23**, 2228 (2009)
17. D.L. Platus, *Negative-stiffness-mechanism vibration isolation systems*, SPIE proceedings, Vibration Control in Microelectronics, Optics, and Metrology **1619**, 44 (1991)
18. W.S. Robertson, M.R.F. Kidner, B.S. Cazzolato, A.C. Zander, J. Sound Vibr. **326**, 88 (2009)
19. W. Robertson, B. Cazzolato, A. Zander, J. Sound Vib. **331**, 1331 (2012)
20. C.V. Jutte, S. Kota, J. Mech. Design **130** (2008)
21. C.V. Jutte, S. Kota, J. Mech. Design **132** (2010)
22. S. Keye, R. Keimer, S. Homann, Aerospace Sci. Technol. **13**, 165 (2009)
23. F. Mattioni, P.M. Weaver, K.D. Potter, M.I. Friswell, Int. J. Solids Struct. **45**, 657 (2008)

24. A. Carrella, M.I. Friswell, *A passive vibration isolator incorporating a composite bistable plate*, in *ENOC 08*, St. Petersburg, Russia, 30 June–4 July 2008
25. A. Carrella, M.I. Friswell, A. Pirrera, G.S. Aglietti, *Numerical and experimental analysis of a square bistable plate*, in *ISMA 08*, Leuven, Belgium, 15–17 September 2008
26. L. Kela, P. Vahaoja, Appl. Mech. Rev. **62**, 060801 (2009)
27. C.G. Diaconu, P.M. Weaver, F. Mattioni, Thin-Walled Struct. **46**, 689 (2008)